

Ab Initio Structure Determination of a Small-Pore Framework Sodium Stannosilicate

Artur Ferreira,[†] Zhi Lin,[‡] João Rocha,^{*,‡} Cláudia M. Morais,[‡] Marta Lopes,[‡] and Christian Fernandez[#]

ESTGA, University of Aveiro, 3810-193 Aveiro, Portugal, Department of Chemistry, University of Aveiro, 3810-193 Aveiro, Portugal, Laboratoire Catalyse and Spectrochimie (CNRS UMR6506) ISMRA/Université de Caen, 6 Boulevard du Marechal Juin 14050 Caen

Received November 14, 2000

The structure of a small-pore framework sodium stannosilicate $\text{Na}_2\text{SnSi}_3\text{O}_9 \cdot 2\text{H}_2\text{O}$ (AV-10) has been determined ab initio from powder X-ray diffraction data (XRD). The unit cell is orthorhombic (space group $C222_1$, $Z = 4$) with cell dimensions $a = 7.9453(5)$, $b = 10.3439(7)$, $c = 11.6252(7)$ Å, $V = 955$ Å³. The structure of AV-10 is composed of corner sharing SnO_6 octahedra and SiO_4 tetrahedra, forming a three-dimensional framework structure. The SiO_4 tetrahedra form helix chains along [001] interconnected by SnO_6 octahedra. The SnO_6 octahedra are isolated by SiO_4 tetrahedra and, thus, there are no Sn–O–Sn linkages. AV-10 has been characterized by chemical analysis, powder XRD, scanning electron microscopy, ²⁹Si, ¹¹⁹Sn, single- and (FAM) triple-quantum ²³Na MAS NMR spectroscopy, thermogravimetry (TGA), and nitrogen adsorption isotherms. The zeolitic water of AV-10 is reversibly lost. The dehydrated material has been studied in situ by powder XRD, TGA, and, in particular, triple-quantum ²³Na MAS NMR.

Introduction

The synthesis of inorganic microporous framework solids possessing structures which consist of interconnected octahedral- and tetrahedral-oxide polyhedra is presently raising considerable interest. We have been particularly concerned with the chemistry of microporous titanium and zirconium silicates containing tetracoordinated Si^{4+} and Ti^{4+} or Zr^{4+} , usually in octahedral coordination.^{1–4} We have now extended our work to stannosilicates. Tin was chosen due to its tendency for 6-fold coordination, adequate atomic radius, and because it is amenable to spectroscopic characterization.

Several stannosilicate minerals are known and a few (dense) stannosilicate phases have been crystallized from hydrothermal conditions (ref 5 and refs therein). Despite this, very little work is presently available on the synthesis of microporous stannosilicates. Two microporous and a layered stannosilicate have been reported by Corcoran et al.⁵ Subsequently, Dyer and Jafar reported the synthesis of a third microporous stannosilicate.^{6,7} The structure of all these materials is, however, unknown. Very recently, we reported the synthesis and structural characterization

of small-pore stannosilicates AV-6 and AV-7 which possess the structure of the zirconosilicate minerals umbite⁸ and kostylevite,⁹ respectively. Here, we wish to report the synthesis and structural characterization by a range of techniques of a new sodium stannosilicate (named AV-10, Aveiro microporous solid no.10).

Experimental Section

AV-10 Synthesis. An alkaline solution was made by dissolving 12.28 g of sodium metasilicate ($\text{Na}_2\text{SiO}_3 \cdot 5\text{H}_2\text{O}$, BDH), 1.00 g of NaOH (Aldrich), and 2.50 g of NaCl into 12.29 g of H_2O . A total of 3.87 g of $\text{SnCl}_4 \cdot 5\text{H}_2\text{O}$ (98 m/m%, Riedel-deHaën) dissolved in 4.00 g of H_2O was added to the alkaline solution with thorough stirring. This gel, with the molar composition 8.5 Na_2O :5.4 SiO_2 :1.0 SnO_2 :1.15 H_2O , was transferred to a Teflon-lined autoclave and treated at 200 °C for 4 days under autogenous pressure without agitation. The product was filtered off, washed at room temperature with distilled water, and dried at 70 °C overnight. Then the obtained off-white powder was treated with a NaOH solution. A typical example was as follows. A total of 2.00 g of the obtained powder and 8.14 g of NaOH solution (2.5 w/w%) were mixed and autoclaved under autogenous pressure without agitation for 5 days. The product was collected in the way described above.

Materials Characterization. Powder XRD data were collected on a X'Pert MPD Philips diffractometer (Cu $K\alpha$ X-radiation) with a curved graphite monochromator, a fixed divergence slit of 0.5°, and a flat plate sample holder, in a Bragg–Brentano para-focusing optics configuration. Intensity data were collected by the step counting method (step 0.02° and time 8 s) in the range 2θ 10–130°. Scanning electron microscope (SEM) images and energy-dispersive X-ray spectrometry (EDS) were recorded on a Hitachi S-4100 microscope. ²³Na, ²⁹Si, and ¹¹⁹Sn NMR spectra were recorded at 105.85, 79.49, and 149.09 MHz, respectively, on an Avance (9.4 T, wide-bore) Bruker spectrometer. ²⁹Si MAS NMR spectra were recorded with 40° pulses, a spinning rate of 5.0 kHz, and 60 s recycle delays. Chemical shifts are quoted in ppm from TMS.

* To whom correspondence should be addressed. Fax: +351 234 370084. Tel: +351 234 370730. E-mail: ROCHA@DQ.UA.PT.

[†] ESTGA, University of Aveiro.

[‡] Department of Chemistry, University of Aveiro.

[#] ISMRA/Université de Caen.

- (1) Anderson, M. W.; Terasaki, O.; Ohsuna, T.; Philippou, A.; Mackay, S. P.; Ferreira, A.; Rocha, J.; Lidin, S. *Nature* **1994**, *367*, 347.
- (2) Rocha, J.; Brandão, P.; Lin, Z.; Esculcas, A. P.; Ferreira, A.; Anderson, M. W. *J. Phys. Chem.* **1996**, *100*, 14978.
- (3) Lin, Z.; Rocha, J.; Brandão, P.; Ferreira, A.; Esculcas, A. P.; Pedrosa de Jesus, J. D.; Philippou, A.; Anderson, M. W. *J. Phys. Chem. B* **1997**, *101*, 7114.
- (4) Lin, Z.; Rocha, J.; Ferreira, P.; Thursfield, A.; Agger, J. R.; Anderson, M. W. *J. Phys. Chem. B* **1999**, *103*, 957.
- (5) Corcoran, E. W., Jr.; Vaughan, D. E. W. *Solid State Ionics*, **1989**, *32/33*, 423.
- (6) Dyer, A.; Jafar, J. J. *J. Chem. Soc., Dalton Trans.* **1990**, 3239.
- (7) Dyer, A.; Jafar, J. *J. Chem. Soc., Dalton Trans.* **1991**, 2639.

(8) Lin, Z.; Rocha, J.; Valente, A. *Chem. Commun.* **1999**, 2489.

(9) Lin, Z.; Rocha, J.; Pedrosa de Jesus, J. D.; Ferreira, A. *J. Mater. Chem.* **2000**, *10*, 1353.

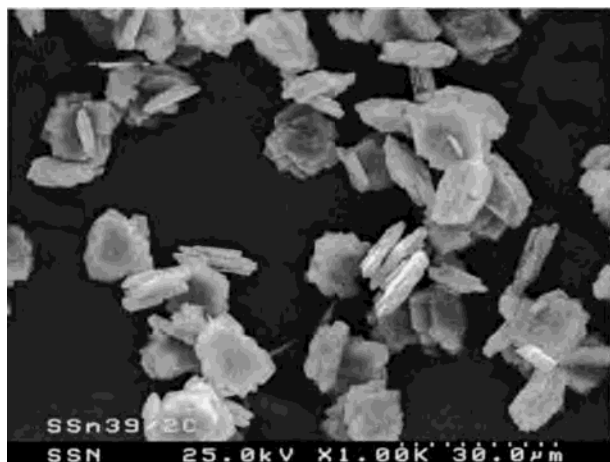


Figure 1. SEM image of AV-10.

Table 1. Conditions of X-ray Data Collection and Refinement for $\text{Na}_2\text{SnSi}_3\text{O}_9 \cdot 2\text{H}_2\text{O}$

Data Collection	
diffractometer, geometry	Philips MPD, Bragg–Brentano
radiation	$\text{CuK}\alpha$
2θ range ($^\circ$)	10.00–130.00
step scan	$0.02^\circ(2\theta)$
time per step	8 s
Results of Rietveld Refinement in $C 222_1 (n 20)$	
Space Group by the FULLPROF Program	
cell parameters (Å)	$a = 7.9453(5)$, $b = 10.3439(7)$, $c = 11.6252(7)$
volume (Å^3)	955.4(1)
formula units/cell (Z)	4
formula Mass (g)	428.97
calculated density (g/cm^3)	2.98
independent reflections/parameters	491/51
peak shape function	Pseudo-Voigt
zeropoint	0.005(2)
halfwidth parameters (U, V, W)	0.090(7), $-0.024(4)$, $0.0243(6)$
asymmetry parameters	0.034(3), $0.041(6)$
transparency correction	0.049(6)
background polynomial parameters	$39.3(9)$, $-5(2)$, $36(8)$, $156(18)$, $39(22)$, $-342(32)$
Reliability Factors (Conventional: Background Excluded)	
for points with Bragg contribution	$R_p = 9.71$, $R_{wp} = 12.8$, $R_{exp} = 6.64$, $\chi^2 = 3.71$
structure reliability factors	$R_B = 4.95$, $R_F = 4.05$

The single-quantum ^{23}Na MAS NMR spectra were measured using short and powerful radio frequency pulses ($0.6 \mu\text{s}$, equivalent to a 15° pulse angle), spinning rates of 32 (AV-10) and 15 (dehydrated AV-10) kHz, and a recycle delay of 2 s. Chemical shifts are quoted in ppm from 1 M aqueous NaCl. The triple-quantum ^{23}Na MAS NMR spectrum of parent AV-10 was recorded using the Z-filter three-pulse sequence.¹⁰ The lengths of the first and second hard pulses (radio frequency magnetic field amplitude $\nu_1 = 250$ kHz) were 2.3 and $0.9 \mu\text{s}$, respectively. The length of the third soft pulse ($\nu_1 = 10$ kHz) was $12.5 \mu\text{s}$. The MAS rate was $\nu_R = 30$ kHz. 128 data points were acquired in the t_1 dimension in increments of $1/\nu_R = 33 \mu\text{s}$. The triple-quantum NMR spectrum of dehydrated AV-10 (400 $^\circ\text{C}$ for 6 h under vacuum) was recorded with a spinning rate of 15 kHz. The lengths of the first and second hard pulses were 3.10 and $1.25 \mu\text{s}$ ($\nu_1 = 130$ kHz). The length of the soft pulse was $12.5 \mu\text{s}$. A total of 332 data points were acquired in the t_1 dimension in increments of $15 \mu\text{s}$. The fast amplitude modulation (FAM) triple-quantum ^{23}Na MAS NMR spectrum was obtained using similar experimental conditions except that the second pulse and the Z-filter pulse were replaced by 4 (X, $-X$, X, $-X$) fast amplitude modulated pulses with a $0.65 \mu\text{s}$ length each.¹¹ The ppm

(10) Amoureux, J.-P.; Fernandez, C.; Steuernagel, S. *J. Magn. Reson.* **1996**, *A123*, 116.

Table 2. Atomic Coordinates and Equivalent Isotropic Displacement Parameters for $\text{Na}_2\text{SnSi}_3\text{O}_9 \cdot 2\text{H}_2\text{O}$

name	x	y	z	U_{eq}^a (Å^2)	site occupation
Sn	0	0.4050(1)	$1/4$	0.022(4)	$1/2$
Si1	0.1872(4)	0.1189(3)	0.2198(2)	0.020(1)	1
Si2	0.3310(6)	0	0	0.009(1)	$1/2$
Na1	0.227(1)	$1/2$	0	0.088(4)	$1/2$
Na2	$1/2$	0.3169(8)	$1/4$	0.056(2)	$1/2$
O1	0.1810(6)	0.2709(4)	0.241(1)	0.035(2)	1
O2	0.0501(8)	0.4089(6)	0.4215(3)	0.028(2)	1
O3	0.3349(6)	0.0439(5)	0.2825(6)	0.022(2)	1
O4	0.2144(8)	0.0858(7)	0.0853(4)	0.036(2)	1
O5	0	0.0648(7)	$1/4$	0.027(3)	$1/2$
Ow	0.437(1)	0.3338(7)	0.0410(6)	0.017(2)	1

^a U_{eq} is defined as one-third of the trace of the orthogonalized U_{ij} tensor.

Table 3. List of Selected Bond Distances (Å) for $\text{Na}_2\text{SnSi}_3\text{O}_9 \cdot 2\text{H}_2\text{O}^a$

bond	distance	bond	distance	bond	distance
Sn–O(3)#1	1.981(6)	Si(1)–O(3)	1.584(6)	Na(1)–OW#7	2.45(1)
Sn–O(3)#2	1.981(6)	Si(1)–O(1)	1.593(6)	Na(1)–OW	2.45(1)
Sn–O(1)#3	2.001(5)	Si(1)–O(4)	1.616(6)	Na(1)–O(2)#8	2.56(1)
Sn–O(1)	2.001(5)	Si(1)–O(5)	1.627(4)	Na(1)–O(2)#3	2.56(1)
Sn–O(2)#3	2.034(4)			Na(1)–O(3)#4	2.615(8)
Sn–O(2)	2.033(4)	Si(2)–O(2)#4	1.617(6)	Na(1)–O(3)#1	2.615(8)
		Si(2)–O(2)#5	1.617(6)		
		Si(2)–O(4)#6	1.621(7)	Na(2)–OW#9	2.487(7)
		Si(2)–O(4)	1.621(7)	Na(2)–OW	2.487(7)
			2.487(7)	Na(2)–O(5)#10	2.56(1)
			2.56(1)	Na(2)–O(1)	2.580(5)
			2.580(5)	Na(2)–O(1)#9	2.580(5)
			2.580(5)		

^a Symmetry transformations used to generate equivalents atoms. #1: $-x + 1/2, y + 1/2, -z + 1/2$. #2: $x - 1/2, y + 1/2, z$. #3: $-x, y, -z + 1/2$. #4: $-x + 1/2, -y + 1/2, z - 1/2$. #5: $-x + 1/2, y - 1/2, -z + 1/2$. #6: $x, -y, -z$. #7: $x, -y + 1, -z$. #8: $-x, -y + 1, z - 1/2$. #9: $-x + 1, y, -z + 1/2$. #10: $x + 1/2, y + 1/2, z$.

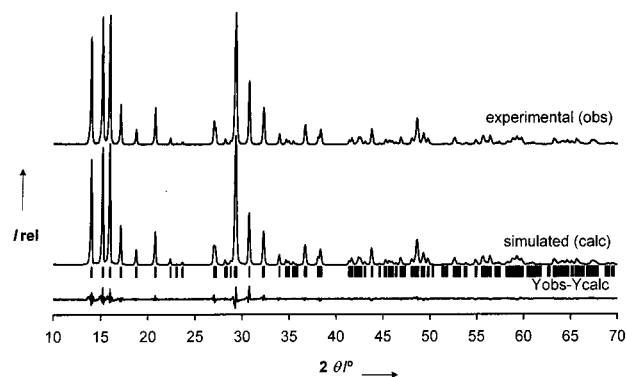


Figure 2. Observed, calculated, and difference powder X-ray diffraction patterns of AV-10.

scale of the sheared spectra was referenced to ν_0 frequency in the ν_2 domain and to $3.78 \nu_0$ in the ν_1 domain (ref 1 M aqueous NaCl).

^{119}Sn MAS NMR spectra were recorded with a 40° pulse, a spinning rate of 14 kHz, and a recycle delay of 100 s. Chemical shifts are quoted in ppm from $\text{Sn}(\text{CH}_3)_4$. Thermogravimetric (TGA) curves were measured with a TGA-50 analyzer. The samples were heated under air at a rate of $5^\circ\text{C}/\text{minute}$. Nitrogen adsorption isotherms were recorded gravimetrically using a CI electronic MK2-M5 microbalance. Equilibrium of each data point was monitored using CI electronics Labweigh software and the pressure was monitored using an Edwards Barocel pressure sensor. The sample was outgassed at 420°C and held at this

(11) Madhu, P. K.; Goldbourt, A.; Frydman, L.; Vega, S. *Chem. Phys. Lett.* **1999**, *307*, 41.

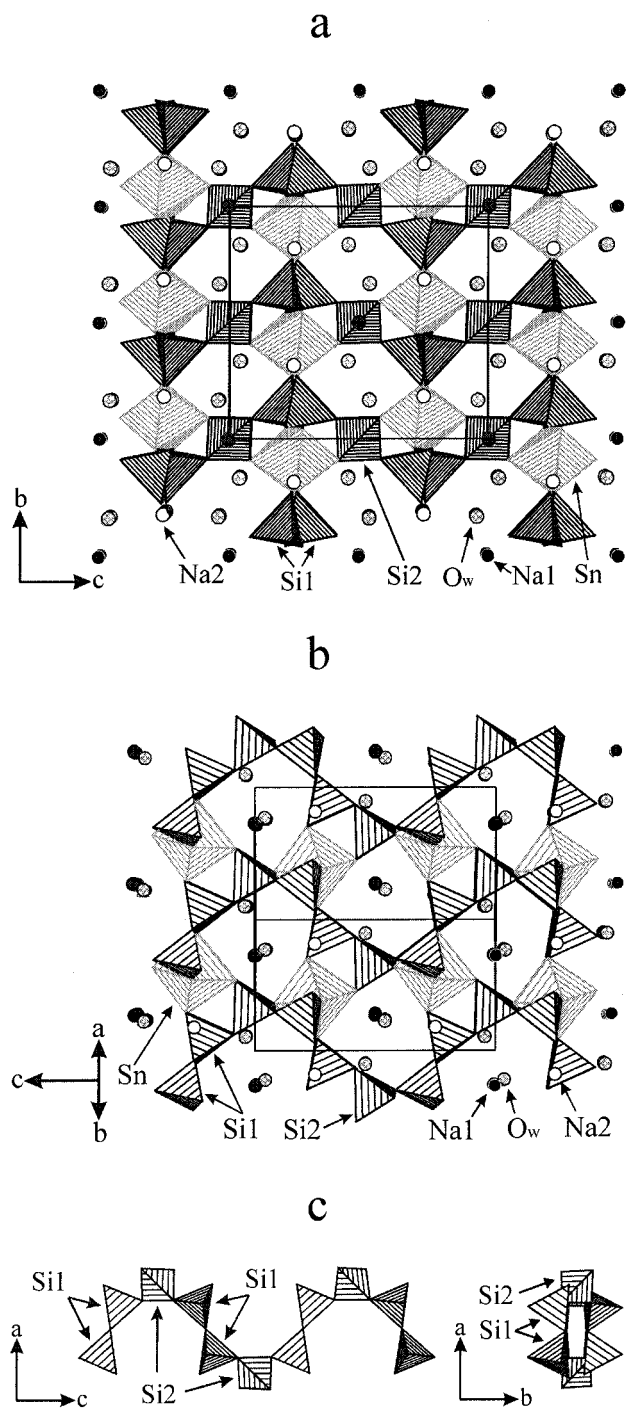


Figure 3. (a,b) Polyhedral representation of the AV-10 structure; (c) the helix chains of SiO₄ tetrahedra in AV-10.

temperature for 14 h, to a residual pressure of ca. 10^{-4} mbar. The specific surface areas (S_{Lang}) were calculated applying the Langmuir equation, with the cross-sectional area of a nitrogen molecule taken as 0.162 nm^2 . The specific total pore volume (V_p) was estimated from the nitrogen uptake at $P/P_0 = 0.95$, using the density of nitrogen in its normal liquid state (0.8081 g cm^{-3}).

Results and Discussion

SEM (Figure 1) shows that AV-10 consists of microcrystalline plates with an average size of ca. $10 \mu\text{m} \times 10 \mu\text{m} \times 2 \mu\text{m}$. Within experimental error, chemical analysis by EDS gave Si/Sn and Na/Sn molar ratios of 3 and 2, respectively. TGA shows that AV-10 loses water in a single step at $200\text{--}250 \text{ }^\circ\text{C}$; the

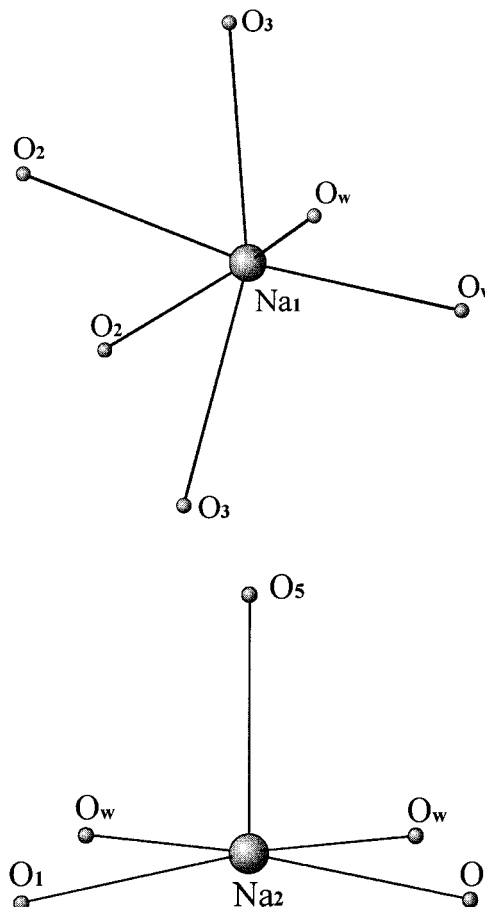


Figure 4. Local environment of Na1 and Na2 in AV-10.

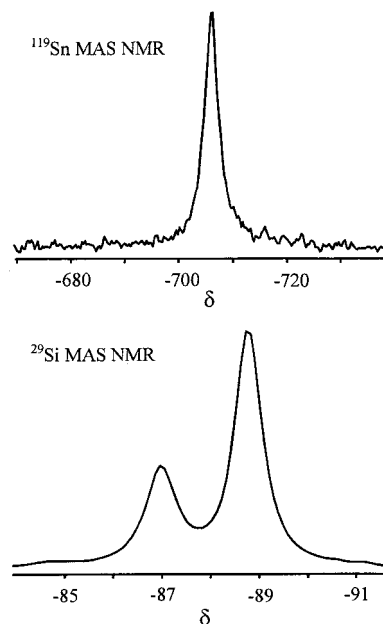


Figure 5. ²⁹Si and ¹¹⁹Sn MAS NMR spectra of AV-10.

total mass loss between 30 and $800 \text{ }^\circ\text{C}$ is ca. 8.6% . Parent AV-10 and a sample calcined to $450 \text{ }^\circ\text{C}$ and rehydrated under air at room temperature for 1 day display identical TGA curves (not shown), thus showing that the water loss is reversible. Powder XRD shows that the framework of AV-10 is stable to, at least, $500 \text{ }^\circ\text{C}$. The AV-10 77 K nitrogen adsorption isotherm (not shown) is of type I, characteristic of a microporous material. The low specific surface area ($S_{\text{Lang}} = 41.6 \text{ m}^2 \text{ g}^{-1}$) and pore

Table 4. List of Selected Bond Angles for Na₂SnSi₃O₉·2H₂O^a

bond	angle (deg)	bond	angle (deg)	bond	angle (deg)
O(3)#1–Sn–O(3)#2	87.1(4)	OW#7–Na(1)–OW	93.7(5)	Si(1)–O(1)–Sn	135.6(3)
O(3)#1–Sn–O(1)#3	171.1(5)	OW#7–Na(1)–O(2)#8	105.0(5)	Si(1)–O(1)–Na(2)	99.1(4)
O(3)#2–Sn–O(1)#3	91.0(4)	OW–Na(1)–O(2)#8	156.3(6)	Sn–O(1)–Na(2)	125.2(2)
O(3)#1–Sn–O(1)	91.0(4)	OW#7–Na(1)–O(2)#3	156.3(6)		
O(3)#2–Sn–O(1)	171.1(5)	OW–Na(1)–O(2)#3	105.0(5)	Si(2)#1–O(2)–Sn	132.8(3)
O(1)#3–Sn–O(1)	92.2(4)	O(2)#8–Na(1)–O(2)#3	61.6(4)	Si(2)#1–O(2)–Na(1)#3	94.9(6)
O(3)#1–Sn–O(2)#3	85.9(4)	OW#7–Na(1)–O(3)#4	93.5(4)	Sn–O(2)–Na(1)#3	100.9(3)
O(3)#2–Sn–O(2)#3	92.5(4)	OW–Na(1)–O(3)#4	101.2(5)		
O(1)#3–Sn–O(2)#3	85.5(5)	O(2)#8–Na(1)–O(3)#4	63.8(3)	Si(1)–O(3)–Sn#11	139.3(3)
O(1)–Sn–O(2)#3	96.1(5)	O(2)#3–Na(1)–O(3)#4	96.9(4)	Si(1)–O(3)–Na(1)#5	113.0(3)
O(3)#1–Sn–O(2)	92.5(4)	OW#7–Na(1)–O(3)#1	101.2(5)	Sn#11–O(3)–Na(1)#5	100.5(3)
O(3)#2–Sn–O(2)	85.9(4)	OW–Na(1)–O(3)#1	93.5(4)		
O(1)#3–Sn–O(2)	96.1(5)	O(2)#8–Na(1)–O(3)#1	96.9(4)	Si(1)–O(4)–Si(2)	141.7(4)
O(1)–Sn–O(2)	85.5(5)	O(2)#3–Na(1)–O(3)#1	63.8(3)		
O(2)#3–Sn–O(2)	177.8(4)	O(3)#4–Na(1)–O(3)#1	158.4(5)	Si(1)–O(5)–Si(1)#3	139.8(3)
				Si(1)–O(5)–Na(2)#12	110.1(5)
O(3)–Si(1)–O(1)	115.7(5)	OW#9–Na(2)–OW	172.0(5)	Si(1)#3–O(5)–Na(2)#12	110.1(5)
O(3)–Si(1)–O(4)	104.0(6)	OW#9–Na(2)–O(5)#10	86.0(4)		
O(1)–Si(1)–O(4)	111.5(8)	OW–Na(2)–O(5)#10	86.0(4)	Na(1)–OW–Na(2)	112.1(4)
O(3)–Si(1)–O(5)	114.2(4)	OW#9–Na(2)–O(1)	104.3(5)		
O(1)–Si(1)–O(5)	106.1(5)	OW–Na(2)–O(1)	77.2(4)		
O(4)–Si(1)–O(5)	105.0(4)	O(5)#10–Na(2)–O(1)	100.6(4)		
		OW#9–Na(2)–O(1)#9	77.2(4)		
O(2)#4–Si(2)–O(2)#5	108.5(5)	OW–Na(2)–O(1)#9	104.3(5)		
O(2)#4–Si(2)–O(4)#6	107.9(6)	O(5)#10–Na(2)–O(1)#9	100.6(4)		
O(2)#5–Si(2)–O(4)#6	111.1(5)	O(1)–Na(2)–O(1)#9	158.7(4)		
O(2)#4–Si(2)–O(4)	111.1(5)				
O(2)#5–Si(2)–O(4)	107.9(6)				
O(4)#6–Si(2)–O(4)	110.3(6)				

^a Symmetry transformations used to generate equivalents atoms. #1: $-x + 1/2, y + 1/2, -z + 1/2$. #2: $x - 1/2, y + 1/2, z$. #3: $-x, y, -z + 1/2$. #4: $-x + 1/2, -y + 1/2, z - 1/2$. #5: $-x + 1/2, y - 1/2, -z + 1/2$. #6: $x, -y, -z$. #7: $x, -y + 1, -z$. #8: $-x, -y + 1, z - 1/2$. #9: $-x + 1, y, -z + 1/2$. #10: $x + 1/2, y + 1/2, z$. #11: $x + 1/2, y - 1/2, z$. #12: $x - 1/2, y - 1/2, z$.

volume ($V_p = 0.015 \text{ cm}^3 \text{ g}^{-1}$) indicate that the pores of this solid are small.

The powder X-ray diffraction pattern of AV-10 was indexed with the PowderX package¹² using the well resolved first 24 lines. The orthorhombic unit cell with $a = 7.946$, $b = 10.3444$, $c = 11.6257 \text{ \AA}$ was indicated by the TREOR90 indexing program¹³ with high figures of merit ($M_{24} = 49$ and $F_{24} = 80$). This result was also confirmed with DICVOL.¹⁴ The best space group suggested by the program Chekcell¹⁵ was $C222_1$ (No. 20). The powder XRD pattern and the unit cell parameters of AV-10 and a previously reported sodium stannosilicate with unknown structure, Sn-A,⁵ are similar. However, the formula reported for Sn-A is $\text{Na}_8\text{Sn}_3\text{Si}_{12}\text{O}_{34} \cdot n\text{H}_2\text{O}$ while the ideal formula of AV-10 is $\text{Na}_2\text{SnSi}_3\text{O}_9 \cdot 2\text{H}_2\text{O}$. It is possible that AV-10 and Sn-A possess the same structure but the latter is probably contaminated with another phase.⁵

The ab initio crystal structure determination from powder XRD data was carried out with the package EXPO.¹⁶ First, the structure factor amplitudes were extracted by the Le Bail method from the powder pattern.¹⁷ The structure factors of 491 reflections were obtained. Then, the structures were solved by

direct methods. Although all atoms were located simultaneously, re-labeling of atoms was necessary, coupled with changes in bond distances and bond angles. This procedure was alternated with least-squares refinements.

The coordinates of atoms obtained from direct methods were used in the Rietveld refinement of the structure by the FullProf program.¹⁸ The final profile analysis refinement was carried out in the range $10\text{--}130^\circ 2\theta$ for the occurring 491 independent reflections and involved the following parameters: structural, 33 atomic coordinates; 11 isotropic temperature factors; profile, one scale factor, three halfwidths (a pseudo-Voigt peak shape function was used), three cell parameters, two peak asymmetry parameters; global, one zero point, six coefficients of polynomial background. Soft constraints to some of the bond distances were applied. Table 1 gives the final crystallographic data for AV-10. The final profile fit is shown in Figure 2, the atomic coordinates are given in Table 2, bond distances and selected bond angles are collected in Tables 3 and 4, respectively.

The framework structure of AV-10 (Figure 3a,b) is made up of SnO_6 octahedra and SiO_4 tetrahedra by sharing corners. Each SnO_6 octahedron shares its corners with six SiO_4 tetrahedra, while each SiO_4 tetrahedron connects to two SnO_6 octahedra and two other SiO_4 tetrahedra. The structure is composed of helix chains of SiO_4 tetrahedra, periodically repeating every six tetrahedra, only two of which are crystallographically non-equivalent with mean Si–O distances of 1.605 and 1.619 \AA (Figure 3c). These chains extend along the [001] direction and are linked by a Sn–O octahedron. Na1 is octahedrally coordinated by four oxygen atoms and two water molecules while

(12) Dong, C. *J. Appl. Crystallogr.* **1999**, *32*, 838.

(13) Werner, P. E.; Eriksson L.; Westdahl, M. *J. Appl. Crystallogr.* **1985**, *18*, 367.

(14) Boulton, A.; Louër, D. *J. Appl. Crystallogr.* **1991**, *21*, 987.

(15) Laugier, J.; Bochu, B. *Programme d'affinement des paramètres de maille à partir d'un diagramme de poudre*, Développé au Laboratoire des Matériaux et du Génie Physique, Ecole Nationale Supérieure de Physique de Grenoble (INPG), Domaine Universitaire BP 46, 38402 Saint Martin d'Hères.

(16) Altomare, A.; Burla, M. C.; Carmalli, M.; Carrozzini, B.; Cascarano, G. L.; Giacovazzo, C.; Guagliardi, A.; Moliterni, A.; Polidori, G.; Rizzi, R. *J. Appl. Crystallogr.* **1998**, *32*, 339.

(17) Le Bail, A.; Duroy, H.; Fourquet, J. L. *Math. Res. Bull.* **1988**, *23*, 447.

(18) Rodriguez-Carvajal, J. *FULLPROF: Program for Rietveld Refinement and Pattern Matching Analysis*; Abstracts of the Satellite Meeting on Powder Diffraction of the XV Congress of the International Union of Crystallography: Toulouse, France, 1990; p 127.

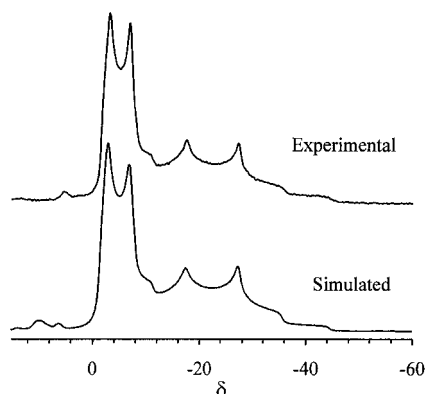


Figure 6. Experimental and simulated single-quantum (“normal”) ^{23}Na MAS NMR spectrum of AV-10.

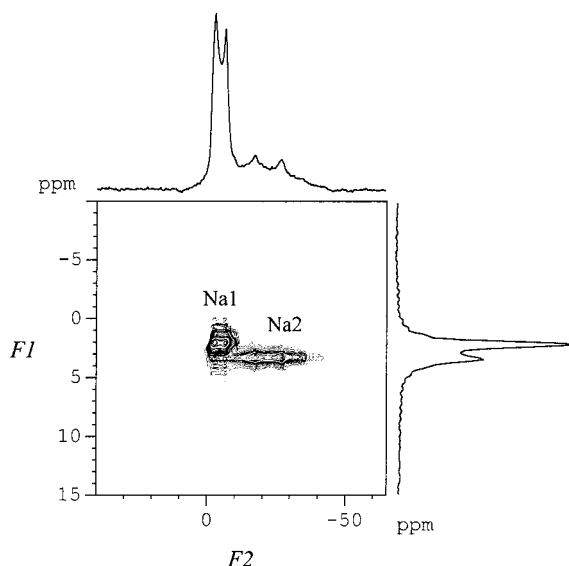


Figure 7. Triple-quantum ^{23}Na MAS NMR spectrum of AV-10. The projection onto axis F2 corresponds to the “normal” ^{23}Na MAS NMR spectrum. The F1 projection is an isotropic spectrum and displays two sharp peaks, revealing the presence in AV-10 of two different Na sites.

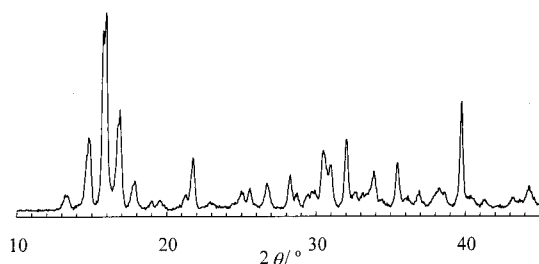


Figure 8. Powder XRD pattern of dehydrated AV-10 recorded in situ at 400 °C under vacuum.

Na2 is pentahedrally coordinated by three oxygen atoms and two water molecules (Figure 4). The water molecules in the octahedron are at adjacent corners, while in the pentahedron the water molecules are at opposite corners. In both polyhedra the Na–H₂O bonds are shorter than the Na–O bonds. The narrow channels in AV-10 run along the [110] and $\bar{1}\bar{1}0$ directions defined by seven-member rings (ca. 2.0 Å × 4.1 Å). The sodium atoms with different local environments and the water species are located in these channels. On the other hand, the six-member ring channel (ca. 1.6 Å × 3.6 Å) runs along the [100] and contains only water molecules.

^{23}Na , ^{29}Si , and ^{119}Sn solid-state NMR data support the structure proposed for AV-10. The ^{29}Si MAS NMR spectrum

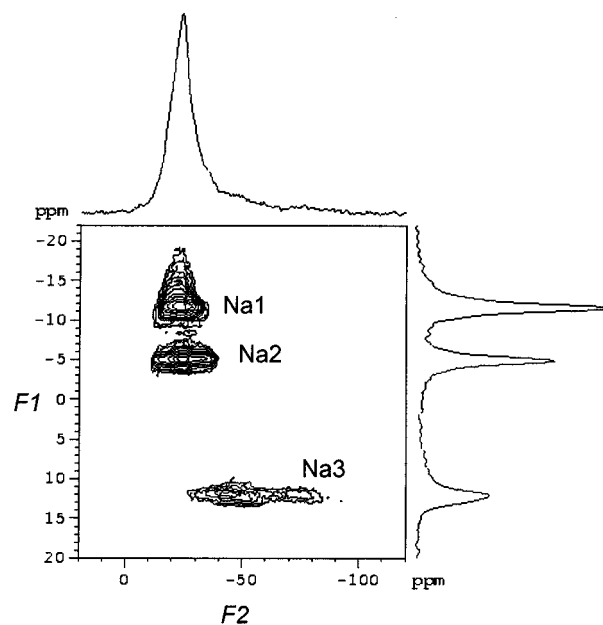


Figure 9. Triple-quantum ^{23}Na MAS NMR spectrum of dehydrated AV-10 (400 °C, under vacuum). The projection onto axis F2 corresponds to the “normal” ^{23}Na MAS NMR spectrum. The F1 projection is an isotropic spectrum and displays three sharp peaks, revealing the presence of three different Na sites.

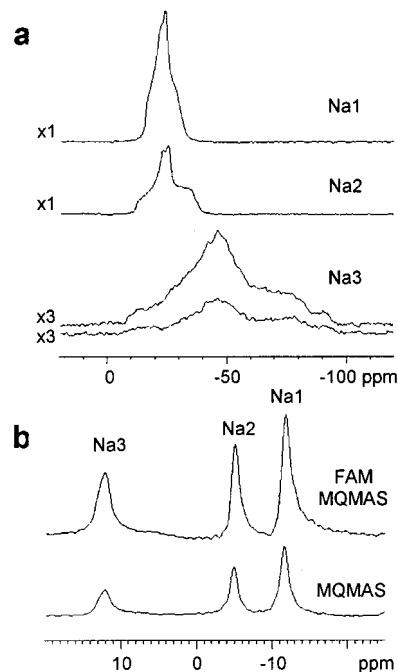


Figure 10. (a) Cross-sections through the three resonances of dehydrated AV-10 show well-defined second-order quadrupole line shapes. For Na3 the (stronger) top line is the FAM spectrum cross-section while the bottom trace is the cross-section of the spectrum in Figure 9. (b) Absolute intensity isotropic F1 projections of the FAM spectrum and Figure 9 triple-quantum spectrum of dehydrated AV-10.

(Figure 5) displays two peaks at ca. –87.0 and –88.7 ppm in a 1:2 intensity ratio. The previously reported Sn-A sample⁵ also gives two resonances in a 1:2 intensity ratio but at ca. –88.5 and –90.3 ppm. In accord with this observation, the crystal structure of AV-10 calls for the presence of two Si(2Si,2Sn) sites with 1:2 populations. Hence, the AV-10 peaks at –87.0 and –88.7 ppm are assigned to Si2 and Si1, respectively. The framework stannosilicates AV-6 and AV-7 give resonances between –84 and –87 ppm.^{8,9}

The ^{119}Sn MAS MNR spectrum of AV-10 (Figure 5) displays a single peak at ca. -706 ppm, with a full-width at half-maximum of ca. 480 Hz, ascribed to the single Sn(6Si) environment present. The Sn-A material⁵ also gives a resonance at -706 ppm. AV-6 and AV-7 give a single peak at ca. -709 ⁸ and -688 ⁹ ppm, respectively.

The single-quantum ("normal") AV-10 ^{23}Na MAS NMR spectrum (Figure 6) displays characteristic second-order quadrupole powder patterns. Triple-quantum ^{23}Na MAS NMR spectroscopy (Figure 7) clearly shows the presence of two different Na sites with rather different quadrupole coupling constants. The simulation of the single-quantum spectrum (Figure 6) assuming the presence of two Na sites yields the following parameters: quadrupole coupling constant 1.40 MHz, asymmetry parameter 0.20 and isotropic chemical shift -0.2 ppm for site Na1 and 2.58 MHz, 0.45, and -6.1 ppm for site Na2. The intensities are in a 1:1 ratio. The pentacoordinated, more distorted, site Na2 probably gives the resonance with the larger quadrupole coupling constant. These results fully support the structure proposed for AV-10.

Upon dehydration the powder XRD pattern of AV-10 changes (Figure 8). Cooling down to room temperature and subsequent rehydration in air (1 d) restores the pattern of the parent material. Although the single-quantum ^{23}Na MAS NMR spectrum of dehydrated AV-10 is poorly resolved, the triple-quantum spectrum (Figure 9) displays three peaks with different quadrupole parameters (Figure 10a), thus showing that the local Na environments change considerably when the zeolitic water is lost. In particular, site Na3 is so distorted that it is difficult to observe in a "normal" MQ MAS experiment. We have, thus, decided to use a recently introduced modification of MQ MAS

spectroscopy known as FAM MQ MAS.¹¹ This technique allows a very efficient conversion of the MQ coherences into single-quantum magnetizations. The FAM pulse sequence parameters were optimized for the observation of the Na3 resonance. As a result, the intensity of this peak increases by a factor of ca. 2.3 relative to the intensity measured in the MQ MAS spectrum and its line shape is less distorted (Figure 10a,b). A preliminary attempt to simulate the single-quantum spectrum of dehydrated AV-10, assuming relative Na populations of 1:1:1, yielded the following parameters: quadrupole coupling constant 1.68 MHz, asymmetry parameter 0.61, and isotropic chemical shift -15.7 ppm, for site Na1, 2.06 MHz, 0.73 and -12.6 ppm, for site Na2, and 3.5 MHz, 0.85 and -8.1 ppm for site Na3. Upon rehydration the spectrum of parent AV-10 is obtained.

In conclusion, we report the synthesis and successful structure determination of AV-10, a small-pore framework sodium stannosilicate. This solid may be of interest in the fields of ion exchange, ionic recognition, and ion conductivity, among others. In view of the interesting ion-exchange properties displayed by previously reported microporous stannosilicates,^{5,7} it is worthwhile to explore the possible applications of AV-10 in ion exchange. This work is now in progress in our laboratory.

Acknowledgment. This work was supported by FCT, POCTI, and FEDER. We thank Dr. Anabela Valente for recording the N_2 adsorption isotherms.

Supporting Information Available: X-ray crystallographic files in CIF format. This material is available free of charge via the Internet at <http://pubs.acs.org>.

IC0012571